Computational Model of DIC Microscopy for Reconstructing 3-D Specimens: From Observations to Measurements.

Farhana Kagalwala and Takeo Kanade

Robotics Institute, Carnegie Mellon University (CMU), Pittsburgh, **PA 15213.**
farhana@cs.cmu.edu, tk@cs.cmu.edu

Frederick Lanni

Center for Light Microscope Imaging and Biotechnology, CMU.
lanni@andrew.cmu.edu

1. SUMMARY

Differential interference contrast (DIC) microscopy, a method pioneered by Georges Nomarski, is widely used to study live biological specimens. However, to date, biologists only qualitatively interpret DIC microscope images. In this work, we describe a method to extract quantitative information from optically-sectioned DIC microscope images. Specifically, given a set of images of a specimen, we attempt to reconstruct the three-dimensional structure and refractive index distribution throughout the specimen.

The nonlinear nature of the DIC imaging process has hindered past attempts at quantitative analysis. Deconvolution of microscope images, also known as computational optical sectioning methods, is restricted to modalities, such as fluorescence. The image intensity, in such modalities, can be approximated as the convolution of a point spread function, or impulse response, with object, source density, or irradiance. In contrast, the image seen in a DIC microscope is an interference image, and therefore the light amplitude has to be modelled, preserving phase information. Within the microscope, an incident light wave is sheared by a prism into two laterally translated wavefronts. The wavefronts travel parallel paths through the specimen, offset by a differential (shear) distance. An interference pattern is detected where the wavefronts recombine.

Our model, a generalized raytracer, uses energy conservation laws to compute the propagation of light through the object and the microscope. After a calibration procedure to obtain prism parameters, we use our model to estimate the specimen's refractive index distribution. We trace rays, the normals to the surfaces of constant phase of the electric field, through inhomogeneous objects. The finite radius of the condenser aperture, and therefore some of the partial coherence of the light, is modelled as well. We compute the diffraction by the lens aperture, and the aberrations caused by the self-occlusion of the specimen to determine the intensity distribution at the image plane. Therefore, we model multiple scatterings through the object, a better approximation than the first Born approximation of light scattered once by the object. Before using the model for the purpose of reconstruction, we validate its use by comparing real and simulated images of known objects. As seen in figures 1 and 2, the model successfully reproduces dominant features of DIC images and defocusing artifacts. Note that the slope of the intensity data, different in the two objects shown, is accurately reproduced in the simulated images.

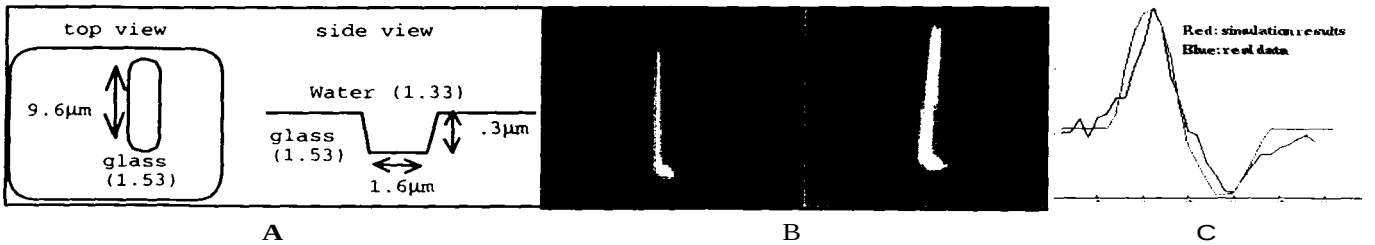

Fig. 1. Comparison of real and simulated images of known specimen. **A:** Schematic of ion-milled wafer. The numbers in brackets are the refractive index values. B-right: real DIC image. B-left: simulated DIC image. C: Superimposed cross-sections from above images.

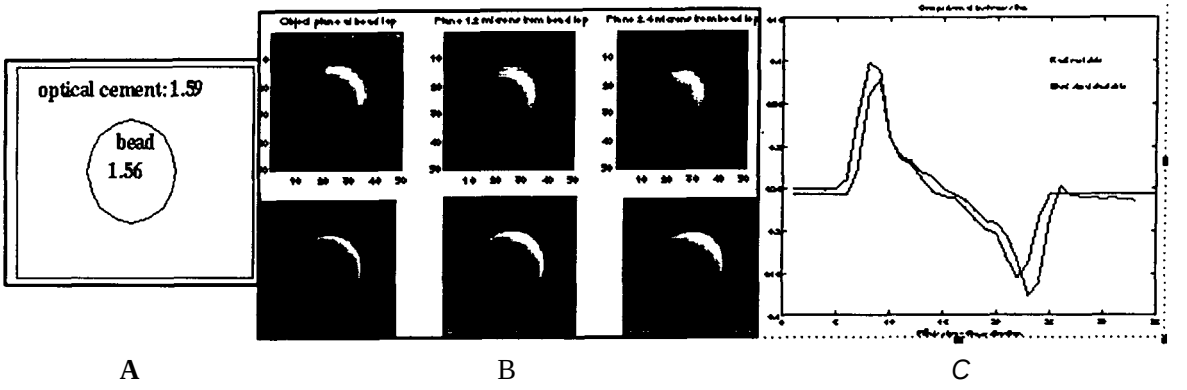

Fig. 2. Comparison of real and simulated images, with specimen 2. A: Schematic of 4pm diameter polystyrene bead immersed in optical cement. The numbers shown are refractive index values. B-top: Actual optically-sectioned DIC images. Leftmost image is focused at bead center, and next images are focused 1μm and 2μm above, respectively. B-bottom: Simulated images at same axial positions **as** above. C: Superimposed cross-sections from the real and simulated leftmost image.

In order to extract the optical properties of the specimen, certain parameters have to be determined. Specifically, we calibrate the relative phase bias and the angular shear, between the two wavefronts of opposite polarization, introduced by the prism. The calibration procedure is based on an analysis of the interference pattern produced by the prism, shown in figure 3. The peak separation determines the angular shear of the prism, and the phase bias can also be computed.

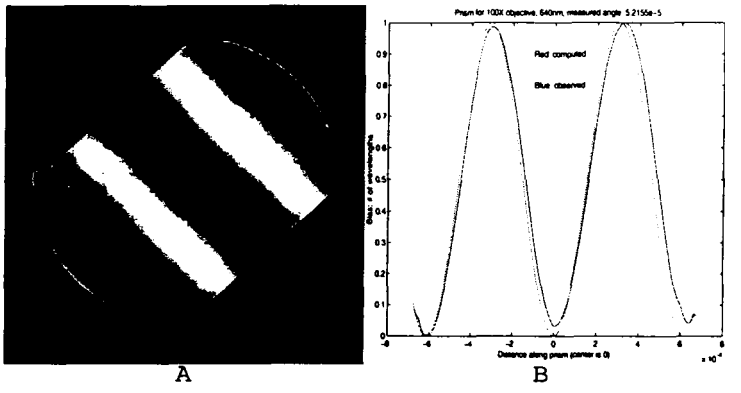

Fig. 3. Interference pattern of Nomarski prism between crossed polarizers. A: Actual image captured by CCD camera. B: Fit of real data to computed pattern after calculating angular shear from the image data.

An iterative non-linear optimization scheme is used to estimate the optical properties and three-dimensional structure of the specimen. Since the degrees of freedom of the system is large, we use a multi- resolution scheme to impose a regularization on the optimization. We represent the refractive-index distribution with respect to a wavelet basis. At each iteration, we estimate more wavelet coefficients, and therefore estimate higher frequency components present in the specimen. To demonstrate that this method can estimate the refractive index distribution, we reconstruct a one-dimensional specimen, **as** shown in figure **4.** Results from higher dimensional specimens are currently being compiled.

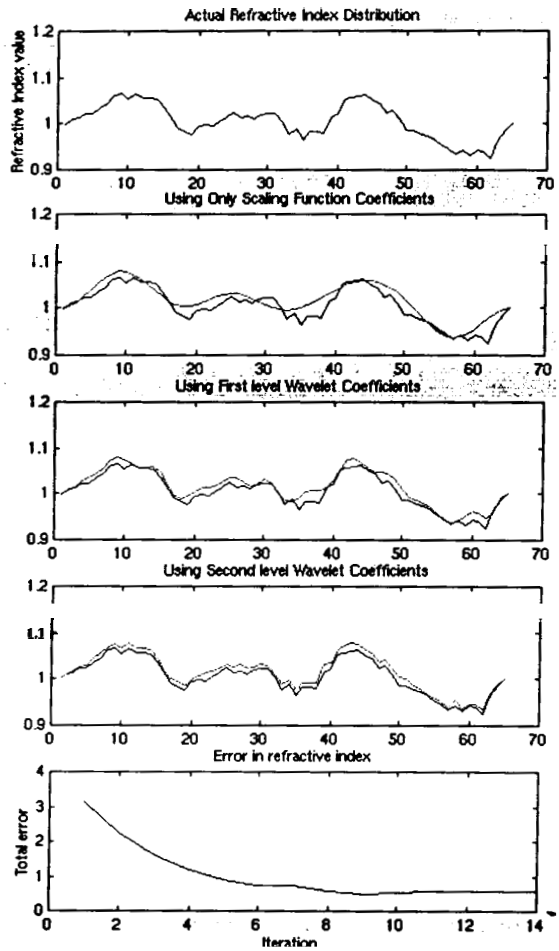

Fig. 4. 1-D reconstruction results. Row 1: Actual refractive index distribution. Rows 2-4: Results after iteration 1-3 respectively. Each plot contains known and estimated refractive index. Row 5: Error between known and estimated refractive index at each iteration.